



OPEN

## Real-time prediction of formation pressure gradient while drilling

Ahmed Abdelaal, Salaheldin Elkatatny✉ & Abdulazeez Abdulraheem

Accurate real-time pore pressure prediction is crucial especially in drilling operations technically and economically. Its prediction will save costs, time and even the right decisions can be taken before problems occur. The available correlations for pore pressure prediction depend on logging data, formation characteristics, and combination of logging and drilling parameters. The objective of this work is to apply artificial neural networks (ANN) and adaptive neuro-fuzzy inference system (ANFIS) to introduce two models to estimate the formation pressure gradient in real-time through the available drilling data. The used parameters include rate of penetration (ROP), mud flow rate (Q), standpipe pressure (SPP), and rotary speed (RS). A data set obtained from some vertical wells was utilized to develop the predictive model. A different set of data was utilized for validating the proposed artificial intelligence (AI) models. Both models forecasted the output with a good correlation coefficient (R) for training and testing. Moreover, the average absolute percentage error (AAPE) did not exceed 2.1%. For validation stage, the developed models estimated the pressure gradient with a good accuracy. This study proves the reliability of the proposed models to estimate the pressure gradient while drilling using drilling data. Moreover, an ANN-based correlation is provided and can be directly used by introducing the optimized weights and biases, whenever the drilling parameters are available, instead of running the ANN model.

### List of symbols

$P_g$	Pressure gradient
ANN	Artificial neural network
ANFIS	Adaptive network-based fuzzy interference system
$R$	Correlation coefficient
AAPE	Average absolute percentage error
AI	Artificial intelligence
FIS	Fuzzy inference system
$R^2$	Coefficient of determination
MSE	Mean squared error
WOB	Weight on bit
RPM	Rotating speed in revolutions per minute
ROP	Rate of penetration
GPM	Gallon per minute
SPP	Standpipe pressure
T	Torque
fitnet	Function fitting neural network
newfit	Create fitting network
newcf	Create cascade-forward backpropagation network
newelm	Create Elman backpropagation network
newlrn	Layer-recurrent network
newtdnn	Create distributed time delay neural network
newff	Create feedforward backpropagation network
newpr	Create pattern recognition network
newftd	Create feedforward input-delay backpropagation network
trainbr	Bayesian regularization
trainoss	One step secant backpropagation
trainlm	Levenberg–Marquardt backpropagation

College of Petroleum Engineering and Geosciences, King Fahd University of Petroleum and Minerals, Dhahran 31261, Saudi Arabia. ✉email: elkatatny@kfupm.edu.sa

trainbfg	BFGS quasi-Newton backpropagation
traingdx	Gradient descent with momentum and adaptive learning rule backpropagation
tansig	Hyperbolic tangent sigmoid transfer function
logsig	Log-sigmoid transfer function
hardlims	Hard-limit transfer function
purelin	Linear transfer function
softmax	Softmax transfer function
tribas	Triangular basis transfer function
satlin	Saturating linear transfer function
netinv	Inverse transfer function
radbas	Radial basis transfer function
$b_1$	Input layer biases
$b_2$	Output layer bias
$w_1$	Weights linking inputs and hidden layer
$w_2$	Weights linking output and hidden layer

### Subscripts

$i$	Index of each neuron in the hidden layer
$n$	Normalized value

Formation pressure is exerted by the fluids within the rock pore space. At certain depth, the normal gradient originates from the saltwater column weight extended from the surface to the point of interest. The deviation from the normal trend can be described as abnormal which can be either subnormal or overpressure<sup>1</sup>. Normal pressure is not constant, and it depends on the amounts of dissolved salts, fluid types, gas presences and temperature gradient. Supernormal or overpressure is the formation pressure exceeding the normal hydrostatic pressure while subnormal pressure is the one that is lower than the normal pressure. Supernormal is created by normal pressure in addition to an extra pressure source. The excess pressure may be attributed to different reasons which may be geological, mechanical, geochemical and combined<sup>2</sup>. Abnormal pressure zones may lead to severe technical and economic issues such as kicks and blowouts. Subnormal pressure may lead to loss of circulation and differential pipe sticking resulting in setting additional casing strings (higher drilling costs)<sup>2</sup>. Accurate real-time formation pressure estimation may provide enhanced well path and casing design, better wellbore stability analysis, effective mud program and reduced overall drilling costs<sup>3,4</sup>.

Formation pressure estimation can be either quantitative or qualitative. Most of these techniques depend on comparing the normal trend lines with the observed ones graphically to pick the anomalous changes that may refer to abnormal pressure zones. The existing techniques in the literature utilized well logs, strata properties and drilling parameters. Hottman and Johnson<sup>5</sup> were the first to estimate the pore pressure based on shale logging data by constructing cross plots that relate the pressure gradient to resistivity ratio or sonic travel time difference between the observed and the normal trend. Matthews and Kelly<sup>6</sup> utilized a semi-log scale for Hottman and Johnson correlation. Pennebaker<sup>7</sup> replaced the sonic travel time difference utilized by Hottman and Johnson<sup>5</sup> with the sonic travel time ratio. The author estimated the pore pressure from an X–Y cross plot like the one belongs to Hottman and Johnson. This technique used a single trendline for a certain rock type globally, but this may not be true for all rock types. Eaton<sup>8</sup> confirmed that formation pressure and overburden pressure gradients affect log-derived properties. As a result, the Hottman and Johnson correlations should be expanded to include overburden stress effect. Eaton<sup>8</sup> proposed an empirical model based on sonic data to predict the pressure gradient in shale formations.

Gardner et al.<sup>9</sup> analysed the data used by Hottman and Johnson and introduced another way to estimate the formation pressure by involving the overburden pressure. Bowers<sup>10</sup> mentioned that a power relationship exists between effective stress and sonic velocity. The author estimated the formation pressure using sonic data after rearranging the power equation and replacing the effective stress with ( $\alpha_V - \text{porepressure}$ ). Shell introduced another sonic-based prediction technique called Tau model by introducing a “Tau” parameter in the equation of the effective stress<sup>11,12</sup>. Foster and Whalen<sup>13</sup> were the first to use the equivalent depth method, a vertical method, to estimate the formation pressure from electrical logging. Moreover, Ham<sup>14</sup> utilized the equivalent depth approach with sonic, resistivity and density to predict the formation pressure and drilling fluid weight needed in Gulf Coast wells. Eaton<sup>15,16</sup> introduced empirical models based on resistivity or conductivity to estimate the pressure gradient in shale using well logging. This method can be fairly used in the sedimentary basins where under-compaction is the main source of overpressure<sup>17,18</sup>. Based on the drawbacks of the solo usage of ROP as an indicator of pore pressure, ROP should be corrected or normalized to consider the variation in different drilling parameters. Bingham<sup>19</sup> proposed the D exponent as an attempt to correct the ROP for the variations in weight on bit (WOB), RS and well diameter. Jordan and Shirley<sup>20</sup> proposed a modification to Bingham approach by introducing another term called  $d_{\text{exp}}$ . Rehm and McClendon<sup>21</sup> adjusted Jordan and Shirley  $d_{\text{exp}}$  by including the effect of drilling fluid density change. Quantitatively, formation pressure can be estimated using  $d_c$  values by Eaton method and ratio method. Eaton<sup>15</sup> and Contreras et al.<sup>22</sup> observed that the corrected  $d_{\text{exp}}$  graph is very analogous to the resistivity graph. Therefore, Eaton developed a prediction model for formation pressure gradient using estimated  $d_c$ , normal  $d_c$  value, and the gradients of overburden and normal formation pressures. The ratio method was proposed as a simple technique to estimate the pore pressure from d exponent or resistivity or sonic data without overburden pressure<sup>1</sup>.

**Artificial intelligence.** AI is an engineering science that uses high computational capabilities to develop computer programs to solve problems by mimicking human brain intelligence<sup>23,24</sup>. AI has different techniques such as ANN, ANFIS, functional networks, and support vector machine that show robust performance and high accuracy for classification and prediction<sup>25</sup>. AI is extensively utilized in different branches of engineering, medicine, economics, and military<sup>26</sup>. AI has been broadly applied in oil and gas industry because it has not only the capability to solve complicated issues, but it also represents them with a high accuracy<sup>27</sup>. Intelligent models were developed for various targets such as estimating the equivalent circulation density in real-time<sup>28–30</sup>, pore pressure estimation while drilling<sup>31,32</sup>, porosity prediction<sup>33</sup>, resistivity prediction<sup>34</sup>, predicting mud rheological properties<sup>35–39</sup>, predicting the unconfined compressive strength<sup>40</sup>, estimating the oil recovery factor<sup>41</sup>, bulk density log prediction<sup>42,43</sup>, well planning<sup>44</sup>, lithology classification<sup>45</sup>, fracture density estimation<sup>46</sup>, estimating the static elastic moduli<sup>47,48</sup>, Poisson's ratio prediction<sup>49–51</sup>, and prediction of formation tops<sup>52</sup>.

**AI-based formation pressure prediction.** Few studies applied different AI techniques to estimate the formation pressure. Li et al.<sup>53</sup> utilized ANN to estimate the formation pressure in the Saertu and Kingshugang oil fields in Daqing. The authors included input parameters like sonic transit time, gamma ray (GR), natural potential, and pipe pressure. Hu et al.<sup>54</sup> employed ANN to estimate the pore pressure. The authors included inputs such as depth, density, sonic transit time, and GR. Keshavarzi and Jahanbakhshi<sup>55</sup> applied neural networks to estimate the gradient in Asmari field. The inputs included porosity, permeability, density, and depth. Aliouane et al.<sup>56</sup> introduced ANN model to estimate the formation pressure from well logs in shale gas reservoir. Rashidi and Asadi<sup>57</sup> proposed ANN model to estimate the formation pressure utilizing mechanical specific energy and drilling efficiency. Ahmed et al.<sup>58</sup> utilized ANN to create a prediction model for formation pressure using seven inputs containing a combination of well logs and drilling data. Ahmed et al.<sup>59</sup> compared five machine learning techniques to predict the formation pressure with the same input parameters utilized in Ahmed et al.<sup>58</sup> work.

The provided models in the literature used some logging data, which may not be available while drilling as logging while drilling (LWD) is not used in all wells. Even if the LWD is present in the drill string, it is placed tens of feet above the bit that does not reflect the instantaneous response of the formations being penetrated in real-time. Other models used some reservoir properties derived from either logging data or lab measurements that limit their usage while drilling. The motivation is to develop a way to forecast the formation pressure gradient in real-time while drilling by using available drilling data only without combining them with other data that are not available in all wells. By doing so, we are maximizing the benefits of the available drilling data without involving higher costs to predict a crucial parameter that enhances the drilling operations technically and economically. The goal of this study is to use ANNs and ANFIS to propose two models for formation pressure gradient prediction in real-time using the available drilling data without additional costs. Moreover, an ANN based correlation is provided to use it directly to estimate the gradient. Unlike the developed empirical equations, the models in this study do not need a normal pressure trend to estimate the gradient.

## Methodology

The methodology started with data collection followed by data cleaning and filtration. Then, data analysis was performed to get more insights about the data sets. After that, data were randomly divided while ensuring that the data sets are representative. The next stage was to select initial model parameters for the first runs. The parameters were updated, and the process was repeated until getting the best results. Once the optimum results came out, the model hyperparameters were extracted. Finally, the models were validated by blind holdout dataset that was not involved in developing the predictive models. Figure 1 briefly shows the methodology conducted in this work to develop the AI models.

## Data processing and analysis

**Data description.** A set of data containing around 3145 points was provided from vertical sections in the same area. The set of data included the drilling data, the formation pressure and depth. The drilling data were utilized as inputs to feed the model to predict the formation pressure gradient as an output. These drilling data included hydraulic data like Q, and SPP, and mechanical data such as: RS, ROP, torque (T), and WOB. These drilling data can be recorded either at surface or downhole while drilling and are influenced by strata being penetrated and their fluid content. Statistical analysis was performed on the field data, and it showed that the data covered a broad range of the inputs and the output as presented in Table 1. For instance, the data had a good representation of the formation pressure gradient as it covers subnormal, normal and supernormal gradient values. Table 2 shows a sample of the field data utilized in this study. The relationship between each variable and the other variables was tested in terms of R as shown in Fig. 2. Moreover, cross-plots of each drilling parameter with pore pressure gradient were constructed as shown in Fig. 3.

**Data processing .** In AI, the quality of data is as significant as the prediction quality. As a result, the data set was cleaned by eliminating the unrepresentative values such as -999 values, and NAN (not a number). Then, the outliers which are the observations located outside the overall pattern of a distribution should be removed because they may cause serious problems in statistical analysis<sup>60</sup>. Outliers may exist owing to human and/or instrument error. Outlier detection can be conducted by many ways such as Z-Score (removing values located away from the mean by more than a certain number of standard deviations) and a box-and-whisker plot (removing values located beyond the upper and the lower limits determined by dividing the data into four quartiles)<sup>61</sup>. The quality and the reliability of the inputs were checked by various techniques like comparing the recorded variables with the ranges of the equipment and with the similar variables in the offset wells within the field. Moreover, the output was compared to the formation pressure gradient values produced by known trends

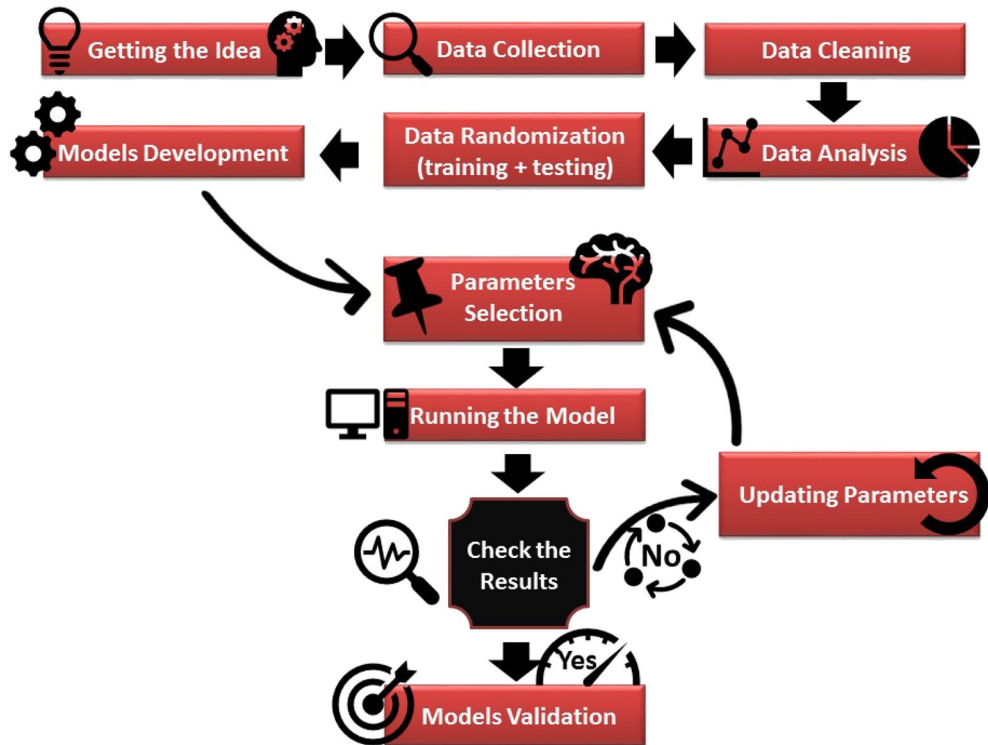


**Figure 1.** Flow chart of the methodology conducted in the study.

Statistical Parameter	Q (gal/min)	SPP (psi)	RS (rpm)	WOB (klb)	T (klb.ft)	ROP (ft/h)	Pressure gradient (psi/ft)
Minimum	283.69	2000.54	65.92	5.21	2.87	3.02	0.36
Maximum	308.83	3140.57	148.96	20.73	5.82	65.08	0.58
Mean	299.52	2599.73	118.73	14.13	3.85	27.22	0.48
Standard deviation	4.53	377.66	22.05	2.38	0.38	9.43	0.08
Skewness	-0.78	0.09	-0.86	-0.10	0.99	0.45	-0.36
Kurtosis	3.55	1.28	2.47	4.44	4.84	3.60	1.36

**Table 1.** Data statistical Analysis.

Pump rate (PR) (gal/min)	SPP (psi)	RS (rpm)	ROP (ft/h)	Pressure gradient (psi/ft)
301.6	2049	70.04	19.27	0.376
301.6	2222	138.23	34.31	0.388
298.0	2271	139.52	24.51	0.477
298.0	2304	141.19	44.61	0.462
298.0	2333	145.67	47.19	0.489
290.8	2778	80.44	29.91	0.568

**Table 2.** A sample of the field data utilized to build the models.

of the gradient of the strata in the selected area. The check showed a good matching between the recorded and produced pressures indicating the reliability of the measurements.

**Selection criteria of the inputs.** The strata characteristics influence the drillability of the geological column because the properties control the impedance to drill through strata. The drilling data may by some means mirror the resistance faced while drilling different formations. Rotary speed and weight on bit can be adjusted based on the nature of the formations<sup>62</sup>. Additionally, the generated cuttings during drilling have impacts on the pressures and rates of the pump required to ensure good hole cleaning. All the previous drilling parameters and

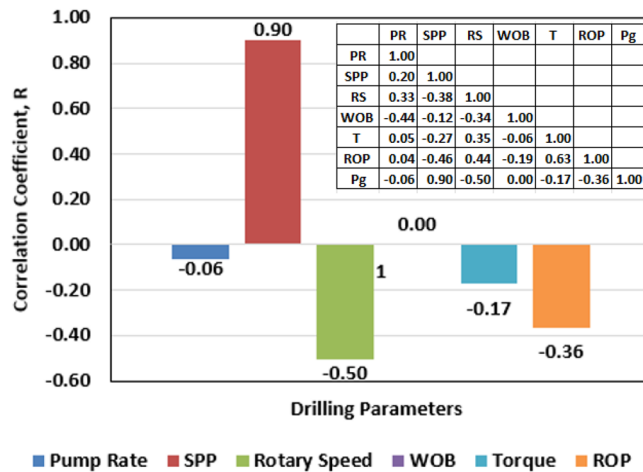


**Figure 2.** R-values between each input and the formation pressure gradient along with a table containing the R-values between each two variables.

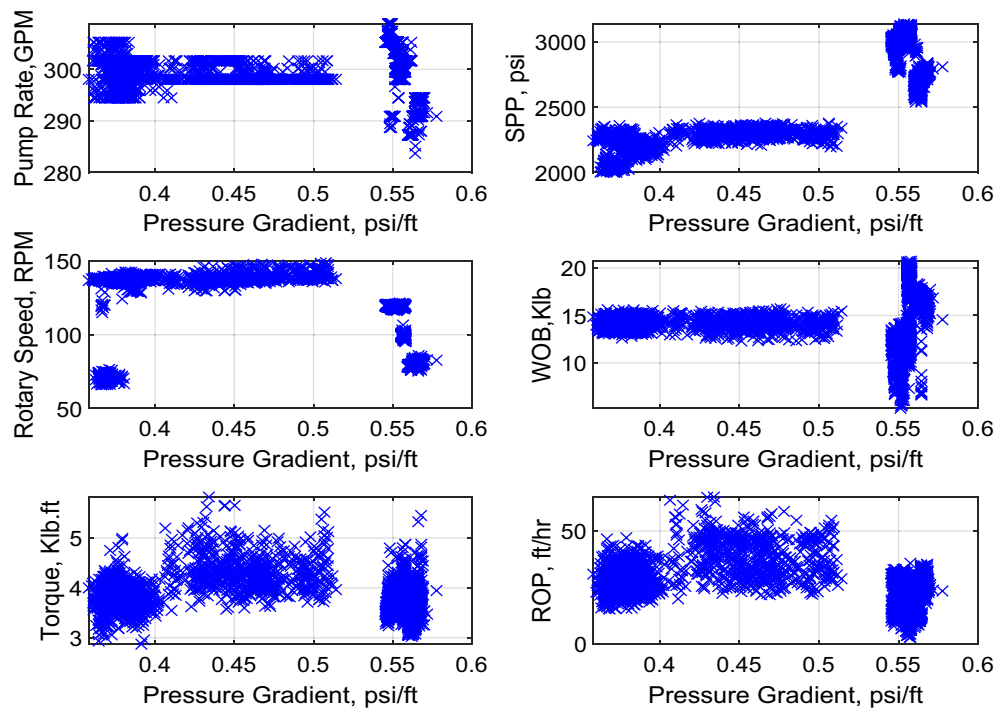


**Figure 3.** Cross-plots of pressure gradient versus different drilling parameters.

the formation type play an important role in controlling penetration rate<sup>63,64</sup>. Consequently, the drilling data can somehow reflect the drilled formations nature, and in turn, their formation pressures. ROP can be used as an indicator to identify supernormal layers while drilling. ROP was included to develop these models since it includes the effect of other drilling variables like WOB. Furthermore, RS was utilized to build the models since it indirectly contains the effect of the T. For the simplicity of the model, two mechanical variables (ROP and RS) were employed along with two hydraulic variables (SPP and Q).

### Development of the pore pressure gradient models

**ANN model.** After checking the quality of the selected dataset. The obtained data had been divided into two groups with 3:1 ratio for training and testing. The ANN model hyperparameters, including different combinations of various available options for ANN hyperparameters, were optimized by testing many scenarios per each parameter. The different options for each ANN parameter and the optimum options are listed in Table 3. The R, coefficient of determination ( $R^2$ ) and AAPE were computed by Eqs. (1), (2) and (3) as presented in Supplemen-



Parameter	Options/range	Optimum option
Hidden layers number	1 to 4	1
Neurons number per each layer	1 to 40	10
Learning rate	0.01 to 0.9	0.12
Network	fitnet–newfit–newlm–newff–newpr–newfftd–newtdnn–newelm–newnarx–newcf	(newcf)
Training function	trainlm–trainbr–traincgb–traincg–trainrp–trainb–trainbr–trainbfg–traincgf–traincgp–traingdx–trainoss–trainr–trainscg	(trainlm)
Transfer function	logsig–satlin–softmax–hardlim–purelin–compet–hardlims–poslin–satlins–radbas–tansig–tribas	(logsig)

**Table 3.** Parameters optimization process.

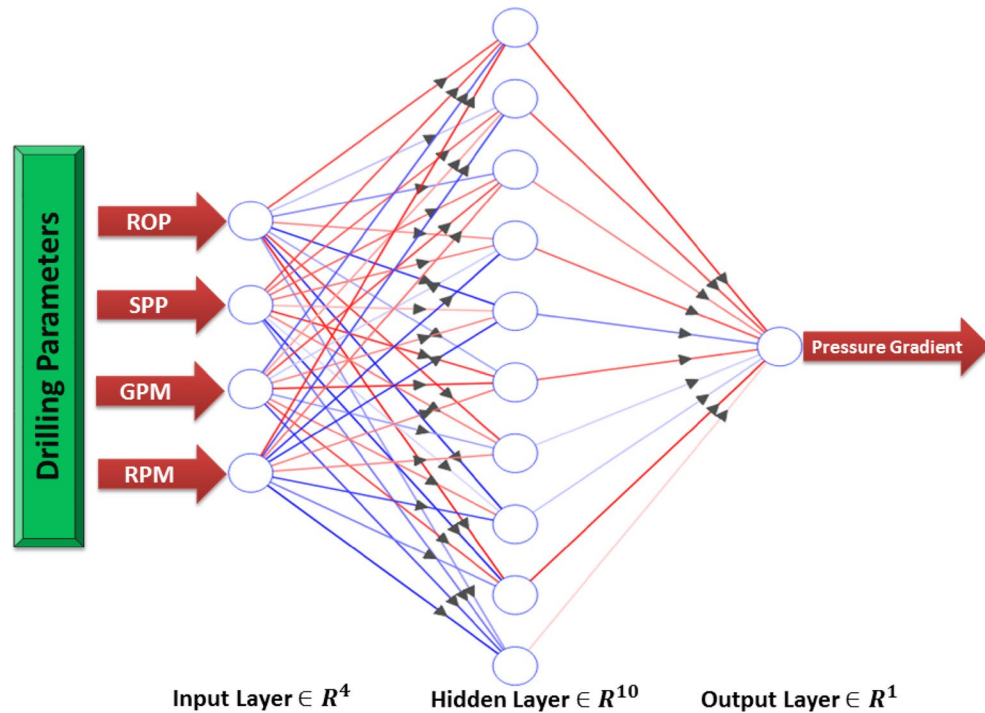


**Figure 4.** Schematic of the structure of the developed ANN.

tary Appendix 1. The hyperparameters providing the highest R, R<sup>2</sup> and the minimum error (RMSE, MSE and AAPE) had been selected. It was found that the optimum number of neurons is 10 occupying only one hidden layer. The model was built using newcf network with Levenberg–Marquardt algorithm (trainlm) as a training function to obtain the optimum weights and biases using 0.12 learning rate. Log-sigmoidal-type (logsig) activation function was used as a transfer function connecting the input and the hidden layer and a linear-type (purelin) activation function linked the hidden and output layers. Figure 4 shows a typical structure of the proposed ANN model.

The proposed ANN model consists of three layers. The first layer contains the inputs; the second layer contains the neurons with their weights and biases and the third layer is the output layer. The input parameters for the model were Q, ROP, SPP and RS. The ANN model predicted the formation pressure gradient with high R of 0.981 and 0.973 for training and testing respectively. Moreover, the RMSE ranges between 0.015 to 0.018 and AAPE does not exceed 2.22% for training and testing. The obtained results for training and testing are summarized in Table 4. The error (predicted—actual) histogram shows that most predicted values have very small error ranging between – 0.02 to 0.02 psi/ft as shown in Fig. 5. The network training performance was monitored against mean squared error as shown in Fig. 6 with the best validation at epoch 48. Figure 7 presents the cross plots of the estimated versus the recorded target values showing the points coinciding with the 45° line. The recorded and predicted target values were graphed on the same plot to observe the variations through the chosen intervals, as presented in Fig. 8, indicating high estimation accuracy.

*New empirical correlation for formation pressure gradient.* The weights and biases were extracted from the optimized ANN model as listed in Table 5 to provide an empirical equation for predicting the pore pressure gradient from the available drilling parameters. The developed equation in the normalized form is given by Eq. (1)

Parameter	Training	Testing
R	0.98	0.97
R <sup>2</sup>	0.96	0.95
AAPE (%)	1.90	2.21
RMSE (psi)	0.015	0.018

**Table 4.** Training and testing results for ANN model.

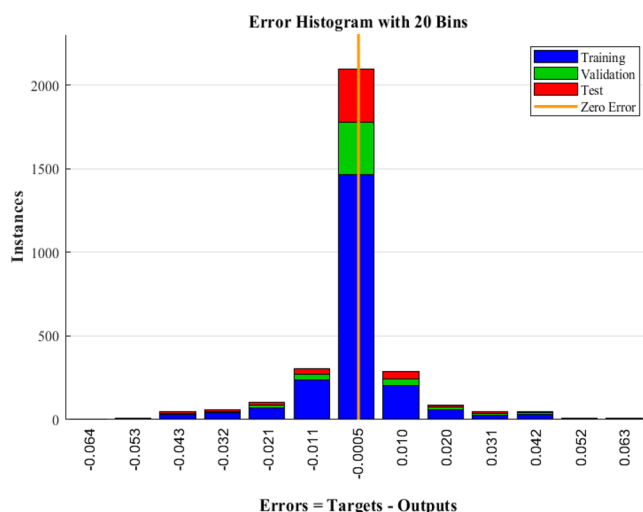


**Figure 5.** Error histogram of the developed ANN model.

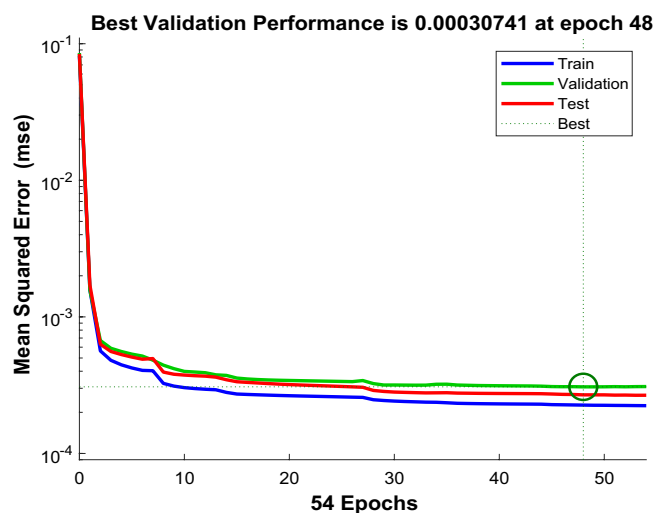


**Figure 6.** Training performance in terms of MSE showing the best validation at epoch 48.

and may be utilized after normalization stage of the input parameters to be in the range of  $-1$  to  $1$  as given by Eq. (2).

$$Pg_n = \left[ \sum_{i=1}^N w_{2_i} \left( \frac{1}{1 + \exp(-(PR_n * w_{1,i,1} + SPP_n * w_{1,i,2} + RS_n + w_{1,i,3} + ROP_n * w_{1,i,4} + b_{1,i}))} \right) \right] + b_2 \tag{1}$$

where  $Pg_n$  is the normalized  $Pg$ ,  $N$  is the neurons number, i.e. 10,  $w_{1_i}$  is the weight associated with each feature between the input and the hidden layer,  $w_{2_i}$  is the weight associated with each feature between the hidden and the output layer,  $b_{1_i}$  is the bias attached to each neuron in the hidden layer,  $b_2$  is bias of the output layer.

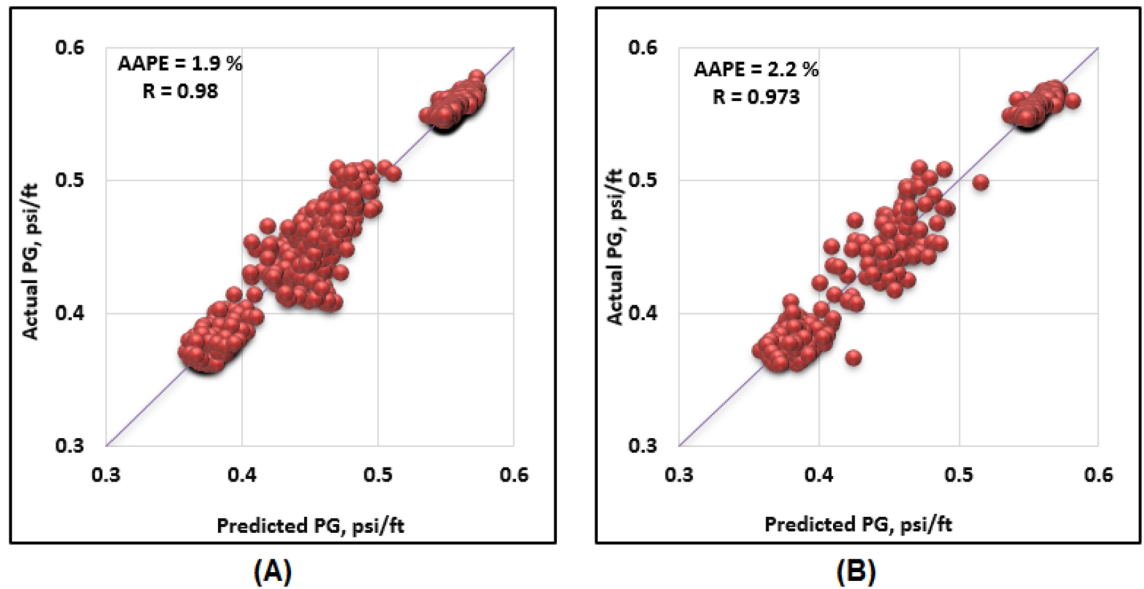


**Figure 7.** Cross-plots of the estimated versus recorded target values (A) training, and (B) testing (ANN model).

$$Y_{i_{nor}} = 2 \left( \frac{Y_i - Y_{i_{min}}}{Y_{i_{max}} - Y_{i_{min}}} \right) - 1 \quad (2)$$

where,  $Y_{i_{nor}}$  is the normalized value of variable  $Y$ ,  $Y_i$  is the value of variable  $Y$  at point  $i$ ,  $Y_{i_{min}}$  is the minimum value of variable  $Y$ ,  $Y_{i_{max}}$  is the maximum value of variable  $Y$ . The minimum and maximum values for each parameter that were used in data normalization are shown in Table 6.

*Steps to estimate the pressure gradient using the ANN-based correlation.*

1. Normalize the input drilling parameters into  $PR_n$ ,  $SPP_n$ ,  $RS_n$  and  $ROP_n$  using Eq. (2) and statistical data in Table 6.
2. Calculate the normalized value of the output  $Pg_n$  using Eq. (1) and the optimum weights and biases listed in Table 5. The input data should be ordered as follows: pump rate (GPM), SPP (psi), rotary speed (RPM) and ROP (ft/h), with the same units.
3. The obtained  $Pg_n$  is denormalized to an actual Pg value by Eq. (3):

$$Pg = 0.11(Pg_n + 1) + 0.36 \quad (3)$$

where,  $Pg_n$  is the normalized Pg estimated by the developed correlation, Pg is the actual value (psi/ft).

**ANFIS model.** ANFIS application in petroleum engineering showed a high reliability as a predictive tool<sup>65</sup>. Genfis 1 that uses grid partitioning and Genfis 2 that uses subtractive clustering were both tested to obtain the model. Genfis 2 provided better results compared to Genfis 1 consequently, the ANFIS model was created by the subtractive clustering technique. The optimization process included using different combinations of cluster radius size and number of iterations. The model was built using the Sugeno–Fis type with a cluster radius of 0.2 and 400 iterations resulting in the best results. The ANFIS model predicted the target with high R of 0.98 and 0.97 for training and testing. Moreover, the RMSE was around 0.02 psi/ft and AAPE does not exceed 2.1% for training and testing. The obtained results for training and testing are summarized in Table 7. Figure 9 presents the cross plots of the predicted versus recorded target values showing the points coinciding with the 45° line. The recorded and estimated values were graphed on the same plot to observe the variations along the chosen intervals, as presented in Fig. 10, indicating high prediction accuracy.

**Models validation.** The proposed ANN and ANFIS models were validated using a blind holdout data set that were not involved in developing the models. A data set (92 points) from the same field was collected to feed the models and compare the recorded versus the estimated pressure gradient values. The models provided continuous profiles of the target using the profiles of the drilling data. Both ANN and ANFIS predicted the target with high R of about 0.99 between the recorded and estimated target values for validation. Additionally, the RMSE was around 0.01 psi/ft and AAPE did not exceed 1.63% for the two models. Figure 11 presents the cross plots of the predicted versus recorded target values showing the points coinciding with the 45° line. The proposed models performed reasonably well when tested using testing and validation data sets that were not included in the training stage.



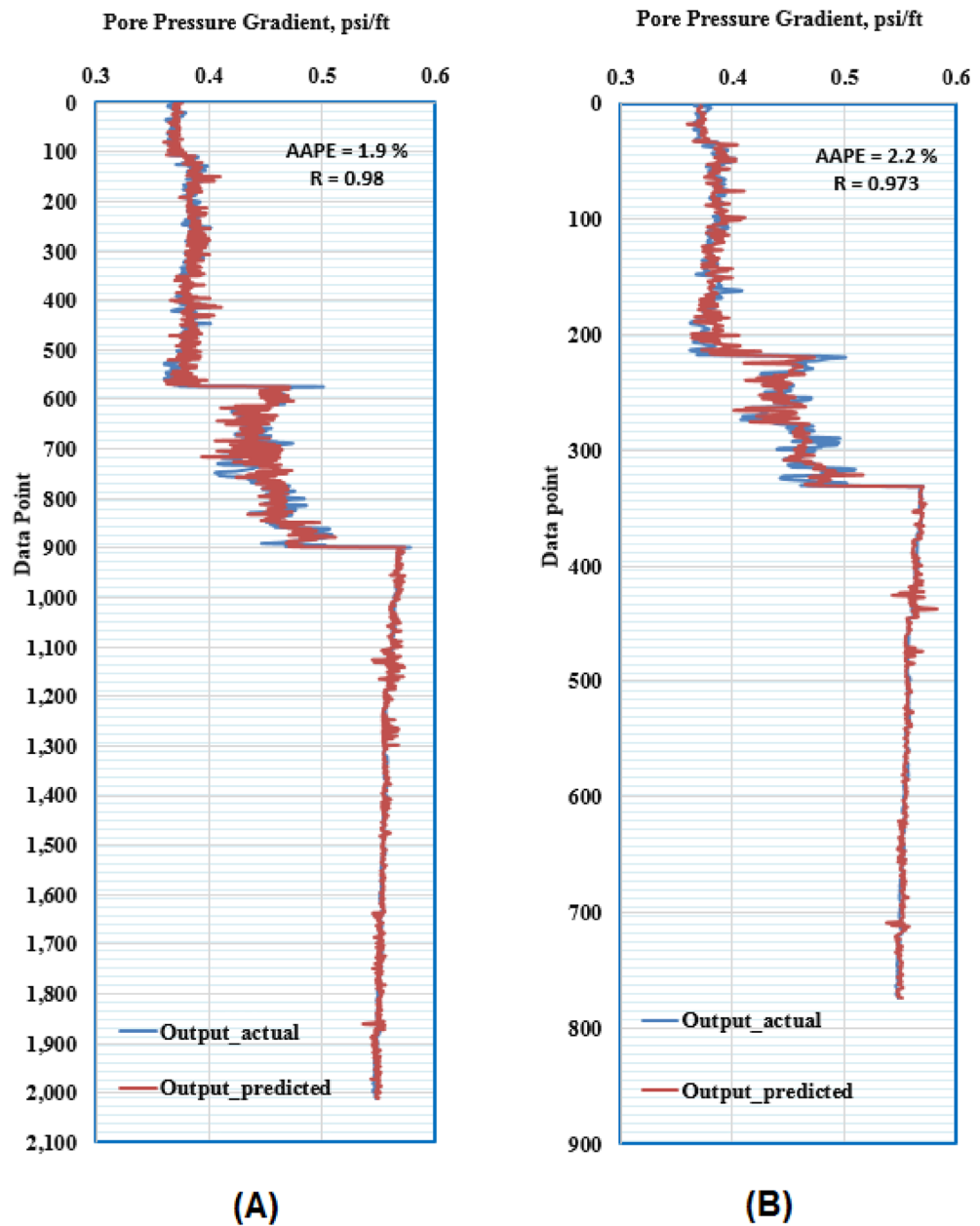


**Figure 8.** Formation pressure gradient profiles (A) training, and (B) testing (ANN model).

Neuron index (i)	$w_1$				$w_2$	$b_1$	$b_2$
	$w_{1,i,1}$	$w_{1,i,2}$	$w_{1,i,3}$	$w_{1,i,4}$			
1	2.5805	-0.1332	-1.5521	2.4388	1.8362	-1.6164	3.5914
2	1.1140	0.3965	-2.0108	2.0790	-1.6815	-2.5735	
3	5.8387	31.5162	5.8181	6.0894	12.2992	0.9777	
4	6.6950	1.9846	6.4276	2.3458	-3.4529	0.4803	
5	0.8564	1.9802	-0.1041	2.1931	-1.7299	3.2192	
6	-6.2878	-4.4130	4.7209	1.6685	-6.8253	5.0057	
7	7.2797	15.3465	-0.6331	-1.6916	4.0337	-2.1368	
8	-3.2785	-10.7832	1.4624	0.7178	-3.0489	-3.1494	
9	-6.7507	-4.1005	2.3319	1.9685	-4.9894	-4.8898	
10	-1.6419	-1.7707	-0.8873	-2.5208	-2.2377	-3.4025	

**Table 5.** Extracted weights and biases for the empirical correlation.

Statistical parameter	Q (gal/min)	SPP (psi)	RS (rpm)	ROP (ft/h)	Pg (psi/ft)
Minimum	283.69	2000.54	65.92	3.02	0.36
Maximum	308.83	3140.57	148.96	65.08	0.58

**Table 6.** Values used for data normalization.

Parameter	Training	Testing
R	0.98	0.97
R <sup>2</sup>	0.96	0.95
AAPE (%)	1.86	2.09
RMSE (psi)	0.016	0.018

**Table 7.** Training and testing results for ANFIS model.

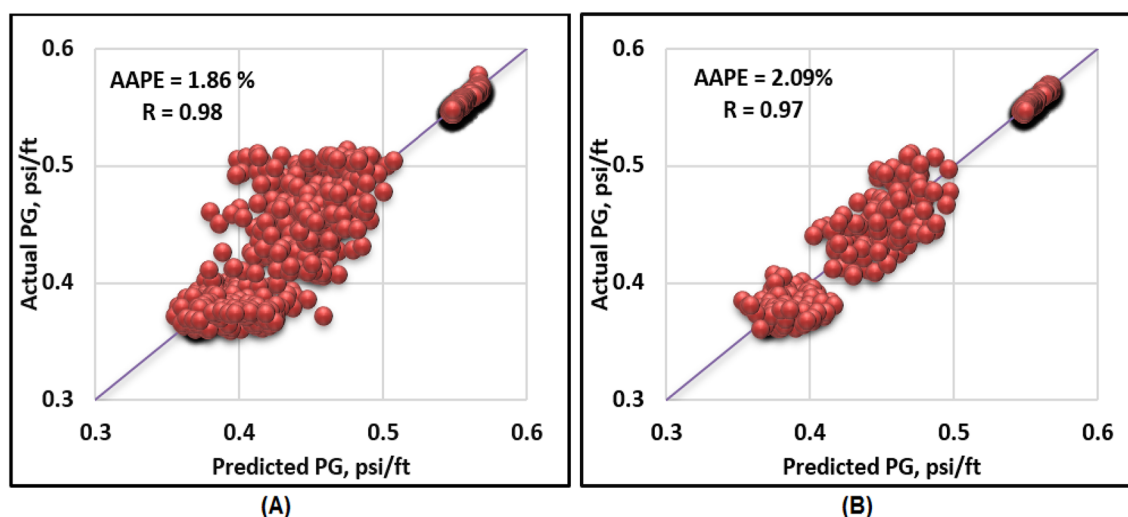


**Figure 9.** Cross-plots of the ANFIS model (A) training, and (B) testing.

## Conclusion

In this work, a novel way for estimating the formation pressure gradient using AI while drilling using the available surface drilling data was introduced. Unlike the developed empirical models in the literature, the developed models do not need a normal trend to predict the formation pressure. The developed models can be merged with any automatic drilling system to estimate the pressure gradient while drilling at low costs. Moreover, it may decrease the non-productive time by minimizing the time-consuming drilling issues by forecasting and minimizing them before they might occur. This tool may improve the drilling operations technically and economically during drilling and pre-drilling design to take the right decisions and to avoid possible issues like kick, blowout, and circulation losses. The results of this work can be listed as follows:

- The optimum parameters of the ANN model are one hidden layer containing 10 neurons, newcf network with Levenberg–Marquardt algorithm (trainlm) as a training function with 0.12 learning rate, and a log-sigmoidal as a transfer function.
- The optimum parameters of the ANFIS model based on subtractive clustering are cluster radius of 0.2, and 400 iterations.
- The proposed models can predict the pore pressure gradient with reasonable accuracy as indicated by R around 0.975, and RMSE around 0.018 psi.
- The ANN-based correlation can be directly utilized by introducing the optimum weights and biases, whenever the drilling parameters are available, instead of running the ANN model.

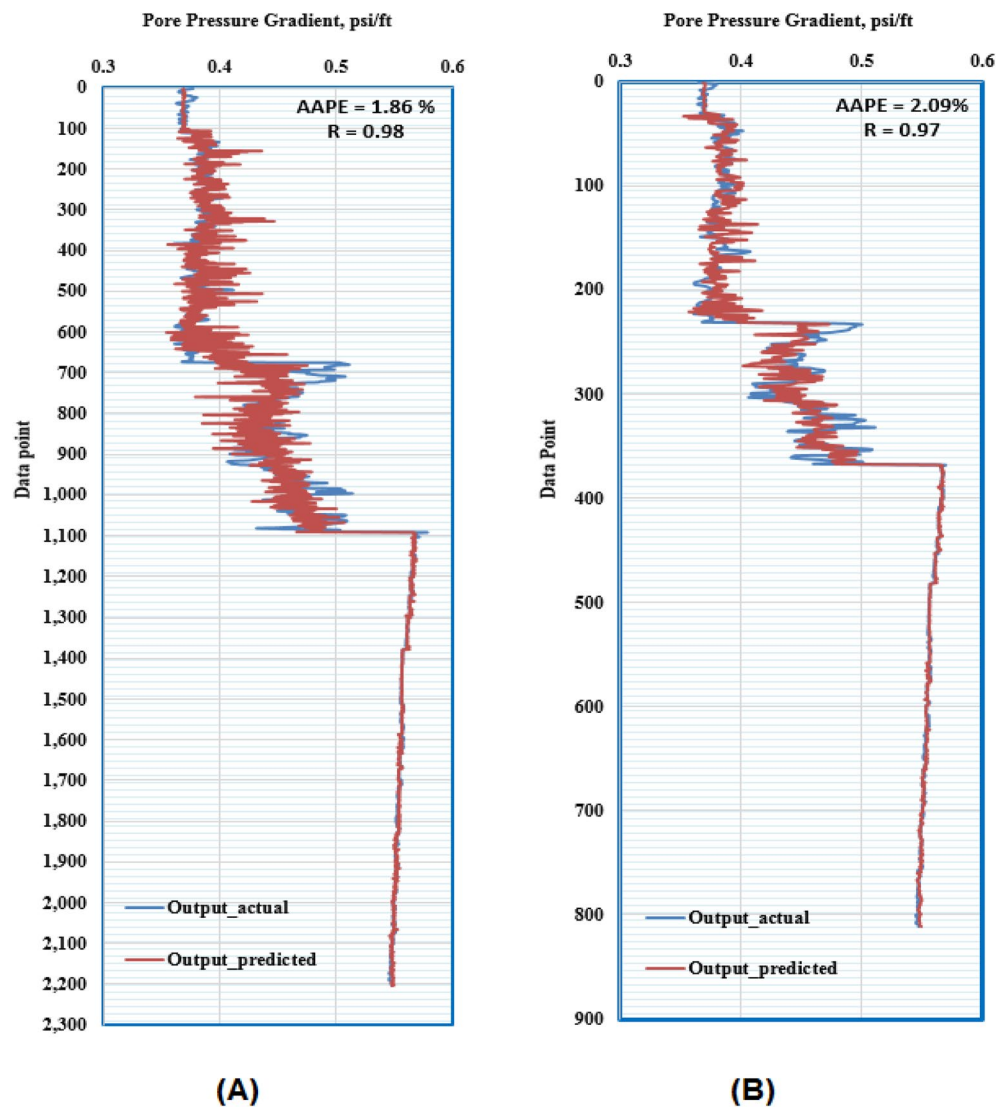


Figure 10. Formation pressure gradient profiles (A) training, and (B) testing (ANFIS model).

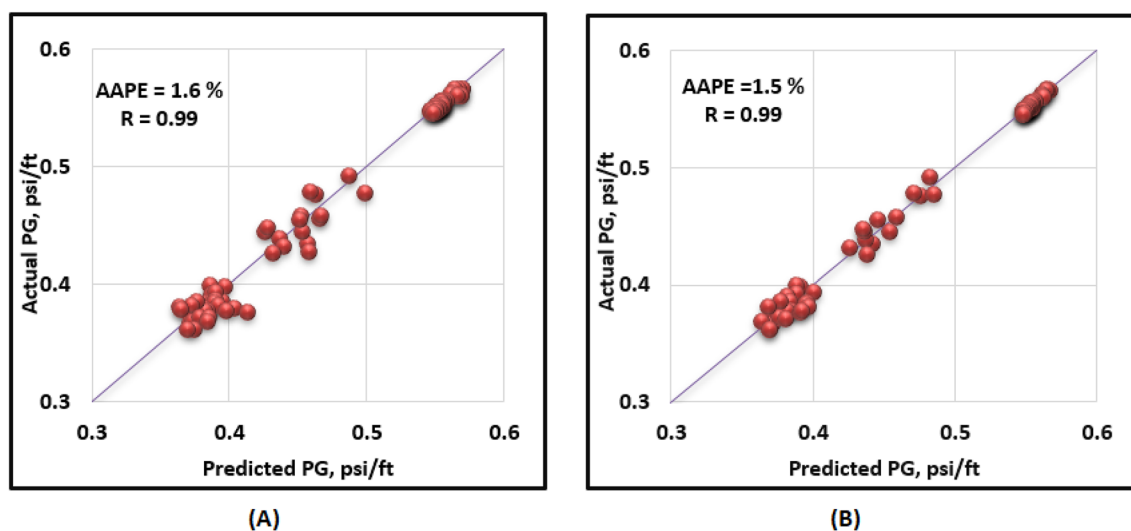


Figure 11. Cross-plots for validation stage (A) ANN, and (B) ANFIS.

Received: 14 April 2022; Accepted: 24 June 2022

Published online: 05 July 2022

## References

- Mouchet, J. P. & Mitchell, A. *Abnormal Pressures While Drilling* (Elf Aquitaine, 1989).
- Rabia, H. *Well Engineering & Construction Hussain Rabia* (Entrac Consulting, 2002).
- Tingay, M. R. P., Hillis, R. R., Swarbrick, R. E., Morley, C. K. & Damit, A. R. Origin of overpressure and pore-pressure prediction in the Baram province, Brunei. *Am. Assoc. Petrol. Geol. Bull.* **93**, 51–74 (2009).
- Zoback, M. D. *Reservoir Geomechanics. Reservoir Geomechanics*. <https://doi.org/10.1017/CBO9780511586477> (Cambridge University Press, 2007).
- Hottman, C. E. & Johnson, R. K. Estimation of formation pressures from log-derived shale properties. *J. Petrol. Technol.* **17**, 1754 (1965).
- Matthews, W. R. & Kelly, J. How to predict formation pressure and fracture gradient from electric and sonic logs. *Oil Gas J.* (1967).
- Pennebaker, E. S. Detection of abnormal-pressure formations from seismic-field data. in *Drilling and Production Practice*. 184–191. (American Petroleum Institute, 1968).
- Eaton, B. A. *The Equation for Geopressure Prediction from Well Logs*. <https://doi.org/10.2118/5544-ms> (Society of Petroleum Engineers (SPE), 1975).
- Gardner, G. H. F., Gardner, L. W. & Gregory, A. R. Formation velocity and density—The diagnostic basics for stratigraphic traps. *Geophysics* **39**, 770–780 (1974).
- Bowers, G. L. Data : Accounting for overpressure mechanisms besides undercompaction. *Soc. Petrol. Eng. (SPE)* **27488**, 89–95 (1995).
- López, J. L., Rappold, P. M., Ugueto, G. A., Wieseneck, J. B. & Vu, C. K. Integrated shared earth model: 3D pore-pressure prediction and uncertainty analysis. *Leading Edge (Tulsa, OK)* **23**, 52–59 (2004).
- Gutierrez, M. A., Braunsdorf, N. R. & Couzens, B. A. Calibration and ranking of pore-pressure prediction models. *Leading Edge (Tulsa, OK)* **25**, 1516–1523 (2006).
- Foster, J. B. & Whalen, H. E. Estimation of formation pressures from electrical surveys—Offshore Louisiana. *SPE Reprint Ser.* **18**, 57–63 (1966).
- Ham, H. H. *A Method of Estimating Formation Pressures from Gulf Coast Well Logs*. Vol. 16. (1966).
- Eaton, B. A. The equation for geopressure prediction from well logs. *OnePetro* <https://doi.org/10.2118/5544-ms> (1975).
- Eaton, B. A. The effect of overburden stress on geopressure prediction from well logs. *J. Petrol. Technol.* **24**, 929–934 (1972).
- Zhang, J. Pore pressure prediction from well logs: Methods, modifications, and new approaches. *Earth Sci. Rev.* **108**, 50–63 (2011).
- Lang, J., Li, S. & Zhang, J. Wellbore stability modeling and real-time surveillance for deepwater drilling to weak bedding planes and depleted reservoirs. in *SPE/IADC Drilling Conference, Proceedings*. Vol. 1. 145–162. (Society of Petroleum Engineers (SPE), 2011).
- Bingham, M. G. A new approach to interpreting rock drillability. *Oil Gas J.* (1965) (**reprinted**).
- Jorden, J. R. & Shirley, O. J. Application of drilling performance data to overpressure detection. *SPE Reprint Ser.* **18**, 19–26 (1967).
- Rehm, B. & McClendon, R. *Measurement of Formation Pressure from Drilling Data*. <https://doi.org/10.2118/3601-ms> (Society of Petroleum Engineers (SPE), 1971).
- Contreras, O., Hareland, G. & Aguilera, R. An innovative approach for pore pressure prediction and drilling optimization in an abnormally subpressured basin. *SPE Drill. Complet.* **27**, 531–545 (2012).
- Kalogirou, S. A. Artificial intelligence for the modeling and control of combustion processes: A review. *Prog. Energy Combust. Sci.* **29**, 515–566 (2003).
- Russell, S. J. & Norvig, P. *Artificial Intelligence: A Modern Approach*. 3rd edn. (2016).
- Mohaghegh, S. Virtual-intelligence applications in petroleum engineering: Part I—Artificial neural networks. *J. Petrol. Technol.* **52**, 64–73 (2000).
- Elsafi, S. H. Artificial neural networks (ANNs) for flood forecasting at Dongola Station in the River Nile, Sudan. *Alex. Eng. J.* **53**, 655–662 (2014).
- Doraisamy, H., Ertekin, T. & Grader, A. S. Key parameters controlling the performance of neuro-simulation applications in field development. in *Proceedings of the SPE Annual Western Regional Meeting*. 233–241. <https://doi.org/10.2118/51079-ms> (Society of Petroleum Engineers (SPE), 1998).
- Alsaihati, A., Elkhatny, S. & Abdulraheem, A. Real-time prediction of equivalent circulation density for horizontal wells using intelligent machines. *ACS Omega* **6**, 934–942 (2021).
- Gamal, H., Abdelaal, A. & Elkhatny, S. Machine learning models for equivalent circulating density prediction from drilling data. *ACS Omega* **8**, 4363 (2021).
- Gamal, H., Abdelaal, A., Alsaihati, A., Elkhatny, S. & Abdulraheem, A. *Artificial Neural Network Model for Predicting the Equivalent Circulating Density from Drilling Parameters*. (2021).
- Abdelaal, A., Elkhatny, S. & Abdulraheem, A. *Formation Pressure Prediction From Mechanical and Hydraulic Drilling Data Using Artificial Neural Networks* (OnePetro, 2021).
- Abdelaal, A., Elkhatny, S. & Abdulraheem, A. Data-driven modeling approach for pore pressure gradient prediction while drilling from drilling parameters. *ACS Omega* <https://doi.org/10.1021/acsomega.1c01340> (2021).
- Gamal, H., Elkhatny, S., Alsaihati, A. & Abdulraheem, A. Intelligent prediction for rock porosity while drilling complex lithology in real time. *Comput. Intell. Neurosci.* **2021**, 14 (2021).
- Abdelaal, A., Ibrahim, A. F. & Elkhatny, S. Data-driven approach for resistivity prediction using artificial intelligence. *J. Energy Resour. Technol.* **144**, 103003 (2022).
- Alsabaa, A. & Elkhatny, S. Improved tracking of the rheological properties of max-bridge oil-based mud using artificial neural networks. *ACS Omega* **6**, 15816–15826 (2021).
- Abdelgawad, K., Elkhatny, S., Moussa, T., Mahmoud, M. & Patil, S. Real-time determination of rheological properties of spud drilling fluids using a hybrid artificial intelligence technique. *J. Energy Resour. Technol. Trans. ASME* **141**, 3 (2019).
- Gowida, A., Elkhatny, S., Ramadan, E. & Abdulraheem, A. Data-driven framework to predict the rheological properties of CaCl<sub>2</sub> brine-based drill-in fluid using artificial neural network. *Energies (Basel)* **12**, 10 (2019).
- Gomaa, I., Elkhatny, S. & Abdulraheem, A. Real-time determination of rheological properties of high over-balanced drilling fluid used for drilling ultra-deep gas wells using artificial neural network. *J. Nat. Gas Sci. Eng.* **77**, 103224 (2020).
- Alsabaa, A., Gamal, H., Elkhatny, S. & Abdulraheem, A. Real-time prediction of rheological properties of invert emulsion mud using adaptive neuro-fuzzy inference system. *Sensors* **20**, 1669 (2020).
- Gowida, A., Elkhatny, S. & Gamal, H. Unconfined compressive strength (UCS) prediction in real-time while drilling using artificial intelligence tools. *Neural Comput. Appl.* <https://doi.org/10.1007/s00521-020-05546-7> (2021).
- Mahmoud, A., Elkhatny, S., Chen, W. & Abdulraheem, A. Estimation of oil recovery factor for water drive sandy reservoirs through applications of artificial intelligence. *Energies (Basel)* **12**, 3671 (2019).
- Ahmed, A., Elkhatny, S., Gamal, H. & Abdulraheem, A. Artificial intelligence models for real-time bulk density prediction of vertical complex lithology using the drilling parameters. *Arab. J. Sci. Eng.* <https://doi.org/10.1007/S13369-021-05537-3> (2021).

43. Gowida, A., Elkatatny, S. & Abdurraheem, A. Application of artificial neural network to predict formation bulk density while drilling. *Petrophysics* **60**, 660–674 (2019).
44. Fatehi, M. & Asadi, H. H. Data integration modeling applied to drill hole planning through semi-supervised learning: A case study from the Dalli Cu-Au porphyry deposit in the central Iran. *J. Afr. Earth Sc.* **128**, 147–160 (2017).
45. Moazzeni, A. & Haffar, M. A. Artificial intelligence for lithology identification through real-time drilling data. *J. Earth Sci. Clim. Change* **06**, 1–4 (2015).
46. Zazoun, R. S. Fracture density estimation from core and conventional well logs data using artificial neural networks: The Cambro-Ordovician reservoir of Mesdar oil field, Algeria. *J. Afr. Earth Sc.* **83**, 55–73 (2013).
47. Siddig, O. & Elkatatny, S. Workflow to build a continuous static elastic moduli profile from the drilling data using artificial intelligence techniques. *J. Petrol. Explor. Product. Technol.* **11**, 3713–3722 (2021).
48. Siddig, O. M., Al-Afnan, S. F., Elkatatny, S. M. & Abdurraheem, A. Drilling data-based approach to build a continuous static elastic moduli profile utilizing artificial intelligence techniques. *J. Energy Resour. Technol.* **144**, 2 (2022).
49. Ahmed, A., Elkatatny, S. & Alsaihati, A. Applications of artificial intelligence for static Poisson's ratio prediction while drilling. *Comput. Intell. Neurosci.* **2021**, 10081 (2021).
50. Siddig, O., Gamal, H., Elkatatny, S. & Abdurraheem, A. Applying different artificial intelligence techniques in dynamic Poisson's ratio prediction using drilling parameters. *J. Energy Resour. Technol.* **144**, 7 (2022).
51. Siddig, O., Gamal, H., Elkatatny, S. & Abdurraheem, A. Real-time prediction of Poisson's ratio from drilling parameters using machine learning tools. *Sci. Rep.* **11**, 1–13 (2021).
52. Al-Abdul Jabbar, A., Elkatatny, S., Mahmoud, M. & Abdurraheem, A. Predicting formation tops while drilling using artificial intelligence. in *Society of Petroleum Engineers-SPE Kingdom of Saudi Arabia Annual Technical Symposium and Exhibition 2018, SATS 2018*. <https://doi.org/10.2118/192345-ms> (Society of Petroleum Engineers, 2018).
53. Li, W., Yan, T. & Liang, Y. Pressure prediction technology of the deep strata based On BP neural network. in *Advanced Materials Research*. Vol. 143–144. 28–31. (Trans Tech Publications Ltd, 2010).
54. Hu, L. *et al.* A new pore pressure prediction method-back propagation artificial neural network. *Electron. J. Geotech. Eng.* **18**, 4093–4107 (2013).
55. Keshavarzi, R. & Jahanbakhshi, R. Real-time prediction of pore pressure gradient through an artificial intelligence approach: A case study from one of middle east oil fields. *Eur. J. Environ. Civ. Eng.* **17**, 675–686 (2013).
56. Aliouane, L., Ouadfeul, S.-A. & Boudella, A. Pore pressure prediction in shale gas reservoirs using neural network and fuzzy logic with an application to Barnett Shale. *EGUGA* **17**, 2723 (2015).
57. Rashidi, M. & Asadi, A. An artificial intelligence approach in estimation of formation pore pressure by critical drilling data. in *52nd U.S. Rock Mechanics/Geomechanics Symposium* (2018).
58. Ahmed, A., Elkatatny, S., Ali, A., Mahmoud, M. & Abdurraheem, A. New model for pore pressure prediction while drilling using artificial neural networks. *Arab. J. Sci. Eng.* **44**, 6079–6088 (2018).
59. Ahmed, A., Elkatatny, S., Ali, A. & Abdurraheem, A. Comparative analysis of artificial intelligence techniques for formation pressure prediction while drilling. *Arab. J. Geosci.* **12**, 7 (2019).
60. Thunder, M., Moore, D. S. & McCabe, G. P. Introduction to the practice of statistics. *Math. Gaz.* **79**, 252 (1995).
61. Dawson, R. How significant is a boxplot outlier?. *J. Stat. Educ.* **19**, 2 (2011).
62. Bourgoyne, J. A. T., Millheim, K. K., Chenevert, M. E. & Young, J. F. S. *Applied Drilling Engineering*. Vol. 2. (1986).
63. Head, A. L. A drillability classification of geological formation. in *World Petroleum Congress Proceedings*. Vol. 1951. 42–57. (One-Petro, 1951).
64. Mensa-Wilmot, G., Calhoun, B. & Perrin, V. P. *Formation Drillability-Definition, Quantification and Contributions to Bit Performance Evaluation*. <https://doi.org/10.2118/57558-ms> (Society of Petroleum Engineers (SPE), 1999).
65. Aghli, G., Moussavi-Harami, R., Mortazavi, S. & Mohammadian, R. Evaluation of new method for estimation of fracture parameters using conventional petrophysical logs and ANFIS in the carbonate heterogeneous reservoirs. *J. Petrol. Sci. Eng.* **172**, 1092–1102 (2019).

## Acknowledgements

The authors would like to thank King Fahd University of Petroleum & Minerals (KFUPM) for permitting the publication of this work.

## Author contributions

S.E. supervised the work, and results analysis. A.A. conducted designed the methodology and data analysis. A.A.Z. also participated in methodology design, and results analysis. The original manuscript was written by A.A. and all authors participated in the manuscript revision and editing.

## Funding

This research received no external funding.

## Competing interests

The authors declare no competing interests.

## Additional information

**Supplementary Information** The online version contains supplementary material available at <https://doi.org/10.1038/s41598-022-15493-z>.

**Correspondence** and requests for materials should be addressed to S.E.

**Reprints and permissions information** is available at [www.nature.com/reprints](http://www.nature.com/reprints).

**Publisher's note** Springer Nature remains neutral with regard to jurisdictional claims in published maps and institutional affiliations.



**Open Access** This article is licensed under a Creative Commons Attribution 4.0 International License, which permits use, sharing, adaptation, distribution and reproduction in any medium or format, as long as you give appropriate credit to the original author(s) and the source, provide a link to the Creative Commons licence, and indicate if changes were made. The images or other third party material in this article are included in the article's Creative Commons licence, unless indicated otherwise in a credit line to the material. If material is not included in the article's Creative Commons licence and your intended use is not permitted by statutory regulation or exceeds the permitted use, you will need to obtain permission directly from the copyright holder. To view a copy of this licence, visit <http://creativecommons.org/licenses/by/4.0/>.

© The Author(s) 2022